Neural Comput & Applic (2013) 22:427–433
DOI 10.1007/s00521-012-0892-7

3D object recognition based on a geometrical topology model and extreme learning machine

Rui Nian · Bo He · Amaury Lendasse

Received: 19 August 2011 / Accepted: 11 February 2012 / Published online: 1 March 2012

Abstract In this paper, one geometrical topology hypothesis is present based on the optimal cognition principle, and the single-hidden layer feedforward neural network with extreme learning machine (ELM) is used for 3D object recognition. It is shown that the proposed approach can identify the inherent distribution and the dependence structure for each 3D object along multiple view angles by evaluating the local topological segments with a dipole topology model and developing the relevant mathematical criterion with ELM algorithm. The ELM ensemble is then used to combine the individual single-hidden layer feedforward neural network of each 3D object for performance improvements. The simulation results have shown the excellent performance and the effectiveness of the developed scheme.

R. Nian · B. He (✉)
College of Information Science and Engineering,
Ocean University of China, Qingdao 266003, China
e-mail: bhe@ouc.edu.cn

R. Nian
e-mail: nianrui_80@163.com

A. Lendasse
Department of Information and Computer Science,
Aalto University, P.O. Box 15400, 00076 Aalto, Finland
e-mail: amaury.lendasse@aalto.fi

A. Lendasse
IKERBASQUE, Basque Foundation for Science,
48011 Bilbao, Spain

A. Lendasse
Computational Intelligence Group, Computer Science Faculty,
University of the Basque Country, Paseo Manuel de Lardizabal,
1, 20018 Donostia-San Sebastián, Spain

Keywords Extreme learning machines · Geometrical topology hypothesis · Optimal cognition principle · Dipole topology

1 Introduction

3D object recognition is one of the most challenging subjects in pattern recognition [1, 2]. Since humans tend to take 2D projections instead of a direct 3D description for the understanding of the characteristics of the real world, 3D object recognition based on 2D image sequence is actually like the human vision system [3–6].

Dating back to the development of 3D object recognition, most approaches focus on the optimal classification principle that simultaneously partition 2D images into a finite number of the known classes [7–13]. Intuitively, the optimal cognition principle is conceived to distinguish one class from all the other possibly existing data in a large number of classes [14, 15], which, from the perspective of visual geometrical analysis, emphasize primarily on the prediction of geometrical properties for the embedding dataset inclusive all the 2D images from 3D object.

So far, artificial neural networks have been extensively adopted to perform 3D object recognition due to their benefits on generalization, flexibility, nonlinearity, fault tolerance, self-organization, adaptive learning, and computation in parallel [8–10]. However, the bottlenecks in the conventional implementations may lead to issues such as overfitting, local minima, time consuming [8]. The work in [16–19] has made a great breakthrough and founded a novel learning framework called extreme learning machine (ELM) in the single-hidden layer feedforward neural networks (SLFNs), which tends to obtain solutions straightforward and provides with the better performance at

extremely fast learning speed with inspiring abilities such that the hidden node parameters can be randomly chosen and the output weights be analytically determined.

In this paper, we develop a scheme of 3D object recognition from 2D image sequence in a geometrical topology model by means of ELM learning algorithm. The rest of the paper is organized as follows: In Sect. 2, the basic of the ELM is outlined. In Sect. 3, the geometrical topology hypothesis is proposed. In Sect. 4, the 3D object recognition with ELM is developed in detail. In Sect. 5, a simulation example is given in support of the developed scheme. Section 6 gives the conclusions.

2 The basics of ELM

Let N be the number of 3D objects $\{O_1, \ldots, O_n, \ldots, O_N\}$, each 3D object O_n consists of M 2D images $\{I_1^n, \ldots, I_m^n, \ldots, I_M^n\}$ that are sampled from the viewing sphere, with I_m^n denoting the mth 2D image of 3D object O_n.

Suppose that there are Q arbitrary distinct training samples $\{I_q, O_q\}_{q=1}^{Q}$, with the input $I_q = [I_{q1}, I_{q2}, \ldots, I_{qd}]^T \in \mathrm{R}^d$ and the expected output $O_q = [O_{q1}, O_{q2}, \ldots, O_{qN}]^T \in \mathrm{R}^N$.

The input and the output relationship of a general SLFN can be described as follows:

$$\boldsymbol{H}\boldsymbol{\beta} = \boldsymbol{O} \tag{1}$$

$$\boldsymbol{H}(\boldsymbol{a}_1, \ldots, \boldsymbol{a}_{\tilde{Q}}, b_1, \ldots, b_{\tilde{Q}}, \boldsymbol{I}_1, \ldots, \boldsymbol{I}_Q) = \begin{bmatrix} g(\boldsymbol{a}_1 \cdot \boldsymbol{I}_1 + b_1) & \cdots & g(\boldsymbol{a}_{\tilde{Q}} \cdot \boldsymbol{I}_1 + b_{\tilde{Q}}) \\ \vdots & g(\boldsymbol{a}_i \cdot \boldsymbol{I}_q + b_i) & \vdots \\ g(\boldsymbol{a}_1 \cdot \boldsymbol{I}_Q + b_1) & \cdots & g(\boldsymbol{a}_{\tilde{Q}} \cdot \boldsymbol{I}_Q + b_{\tilde{Q}}) \end{bmatrix}_{Q \times \tilde{Q}}$$

$$\boldsymbol{\beta} = \begin{bmatrix} \boldsymbol{\beta}_1 & \cdots & \boldsymbol{\beta}_i & \cdots & \boldsymbol{\beta}_{\tilde{Q}} \end{bmatrix}'_{N \times \tilde{Q}},$$
$$\mathbf{O} = \begin{bmatrix} \boldsymbol{O}_1 & \cdots & \boldsymbol{O}_q & \cdots & \boldsymbol{O}_Q \end{bmatrix}'_{N \times Q}$$

where $\mathbf{H}$ is defined as the hidden layer output matrix, $\tilde{Q}$ is the number of hidden nodes, $g(x)$ stands for the activation function, $\boldsymbol{a}_i = [a_{i1}, a_{i2}, \ldots, a_{id}]^T$ is the weight vector connecting the ith hidden node and the input nodes, b_i is the threshold of the ith hidden node, and $\boldsymbol{\beta}_i = [\boldsymbol{\beta}_{i1}, \boldsymbol{\beta}_{i2}, \ldots, \boldsymbol{\beta}_{iN}]^T$ is the weight vector connecting the ith hidden node and the output nodes, then the expected output is

$$\boldsymbol{O}_q = \sum_{i=1}^{\tilde{Q}} \boldsymbol{\beta}_i g_i(\boldsymbol{I}_q) = \sum_{i=1}^{\tilde{Q}} \boldsymbol{\beta}_i g(\boldsymbol{a}_i \cdot \boldsymbol{I}_q + b_i), \quad q = 1, \ldots, Q.$$

Given a standard SLFN with the activation function $g : \mathrm{R} \to \mathrm{R}$ that is infinitely differentiable in any interval, for the parameters $\boldsymbol{a}_i \in \mathrm{R}^d$ and $b_i \in \mathrm{R}$ randomly chosen from any intervals, ELM learning has the following theorems [16, 20].

Theorem 1 *Given Q hidden nodes, according to any continuous probability distribution, then with probability one, the hidden layer output matrix* $\mathbf{H}$ *is invertible and* $||\boldsymbol{H}\boldsymbol{\beta} - \mathbf{O}|| = 0$.

Theorem 2 *Given any small positive value $e > 0$, there exists $\tilde{Q} \leq Q$ such that according to any continuous probability distribution, then with probability one,* $||\boldsymbol{H}_{Q \times \tilde{Q}} \boldsymbol{\beta}_{\tilde{Q} \times N} - \mathbf{O}_{Q \times N}|| \leq e$.

As long as the number of hidden layer nodes is enough, the SLFN with ELM will converge toward any continuous function with the input weights and hidden layer biases randomly assigned, needless of mathematically predetermined internal knowledge, so that the learning process can be simply considered as a linear system and the output weights can be analytically determined through the Moore–Penrose generalized inverse operation of the hidden layer output matrices. The upper bound of the required number of the hidden nodes is the number of the distinct training samples. For the benefit of good generalization, it is usually set as $\tilde{Q} \ll Q$.

3 Geometrical topology

One common nature of 2D images in 3D object recognition is that they have a one-to-one corresponding in the high-dimensional space [9, 21]. The blessing and the curses of dimensionality will inevitably be the main concern. From the visual geometrical analysis, a geometrical topology hypothesis is present here to perform 3D object recognition based on the optimal cognition principle.

3.1 Optimal cognition principle

In nature, the optimal cognition principle virtually claims a solution for the $O_i/\bar{O}_i$ problem, distinguishing one class from all the other existing classes [14, 15], instead of simply dividing 2D images within a given number of classes [7–13]. The task here is to set up appropriate geometrical topology for each 3D object. Let $\boldsymbol{I}^n$ be the embedding dataset inclusive all the 2D images from 3D object O_n, and S^n correspond to the geometrical topology coverage, inspired by the intuition that 2D images are most likely to lie in or close to some lower dimensional manifolds than the ambient dimension would suggest [21–25], it is probable for us to estimate the geometrical properties of 3D object from relatively simple topology manifolds. The recognition process will specify the membership of 2D image by a spatial mapping with respect to the geometrical topology S^n.

3.2 Geometrical topology hypothesis

The selection of appropriate topology manifolds, well fitting for the objective distribution and inherent nature, is vital for 3D object recognition. Based on the general understanding of the topology nature of 3D objects, the characteristics of the mutual dependence among homologous 2D images can be described as follows.

3.2.1 Homologous continuity law

Suppose that the difference between two 2D images from the identical 3D object is changing gradually or not determined by quantum [26], given $I_x^n, I_y^n \in \boldsymbol{I^n}$, $\varepsilon > 0$ and the similarity measure $d(\cdot)$ in a certain metric [27], there must be at least one gradually changing course, or a set $\boldsymbol{J^n}$,

$$J^n = \{I_x^n = I_{x_1}^n, I_{x_2}^n \ldots I_{x_{j-1}}^n, I_{x_j}^n = I_y^n \Big| d(I_{x_m}^n, I_{x_{m+1}}^n) < \varepsilon, \quad \forall m \in [1, j-1], m \in N\} \subset I^n \tag{2}$$

where all the 2D images in the transition process belong to the same 3D object [14]. Figure 1 is a sketch of the homologous continuity law.

The geometrical topology $\boldsymbol{S^n}$ for each 3D object O_n is hereby presented as,

$$S^n = \bigcup_i S_i^n,\ S_i^n = \{I \big| d(I, \psi_i^n) \le r, I \in R^d\}, \qquad \psi_i^n = \{I \Big| \Phi(I, I_x^n, I_y^n) = 0\} \tag{3}$$

where $d(I, \psi_i^n)$ indicates the similarity measure between any arbitrary input I and the given hyper surface ψ_i^n, and $\Phi(I, I_x^n, I_y^n)$ is a function of the dependence structure among the input I as well as 2D images I_x^n and I_y^n.

In virtue of the homologous continuity law, we put forward the dipole topology model as one kind of the local topology segment, indicating the mutual relationships estimated from any random input I with respect to every two adjoining 2D images I_x^n and I_y^n from the identical 3D object O_n in high-dimensional space. Mathematically, one dipole topology could be expressed in the functional form of the joint probabilistic density as follows,

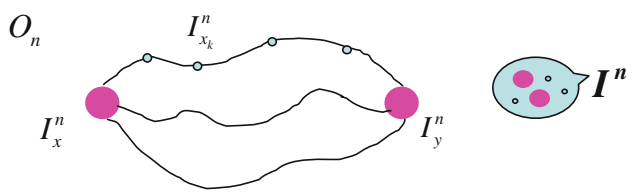

Fig. 1 Homologous continuity law

$$K(I, I_x^n, I_y^n) = hG(I - f(I, I_x^n, I_y^n) \times (I_y^n - I_x^n) \big| I_x^n, \Sigma)$$
$$f(I, I_x^n, I_y^n) = \begin{cases} 0, & \frac{q(I, I_x^n, I_y^n)}{d(I_x^n, I_y^n)} \le 0 \\ 1, & \frac{q(I, I_x^n, I_y^n)}{d(I_x^n, I_y^n)} \ge 1 \\ \frac{q(I, I_x^n, I_y^n)}{d(I_x^n, I_y^n)}, & 0 \le \frac{q(I, I_x^n, I_y^n)}{d(I_x^n, I_y^n)} \le 1 \end{cases} \tag{4}$$

where $G(I|u, \Sigma)$ follows the Gaussian distribution with the mean vector u and the covariance matrix Σ, $G(I|u, \Sigma) = \exp\{-\frac{1}{2}(I-\mu)'\Sigma^{-1}(I-\mu)\} \Big/ (2\pi)^{n/2}|\Sigma|^{1/2}$, $q(I, I_x^n, I_y^n) = (I - I_x^n) \bullet (I_y^n - I_x^n) \Big/ d(I_x^n, I_y^n)$, $d(I_x^n, I_y^n)$ stands for the similarity measure between two 2D images I_x^n and I_y^n, and h denotes the magnitude of the probabilistic distribution. On a set of 2D images along multiple view angles from the identical 3D object in an appropriate order with precise position information, a collection of local topology could be linked as a ring-like structure or a chain-like structure, to trace the geometrical topology for each 3D object.

4 Object recognition

By means of ELM learning, we try to take a further step to facilitate the above geometrical topology model for 3D object recognition in SLFN. For each SLFN, a set of novel neurons will be particularly selected and correspondingly the relevant mathematical criterion will be developed for the dipole topology hypothesis by extending the original ELM strategy. The single SLFN architecture will then be organized into ELM ensemble for combination.

4.1 ELM learning strategy

4.1.1 Neuron model

One general neuron model is introduced here to extend the plain SLFN into multiple weights [14, 15],

$$y = g\left[\sum_{i=1}^{d} \Phi(a_{i1}, a_{i2}, \ldots, a_{im}, I_i) - b\right] \tag{5}$$

where I and y are, respectively, the input and the output, d refers to the dimensionality of the input, b is the bias and $a_{i1}, a_{i2}, \ldots, a_{im}$ consists of m input weights for the neuron, Φ is a function of the dependence structure among the input and multiple weights, g indicates the activation function.

For 3D object recognition, one kind of neurons, coincident with the dipole topology hypothesis, is particularly

chosen here from the general model of SLFN, representing the mapping between one random input I and double points a_1 and a_2. The activation function is taken as $g(I; a_1, a_2, b) = K(I, a_1, a_2, b)$, where a_1 and a_2 are two centers of the neurons, and the bias b is exerted to the relationships among the other three variables.

4.1.2 SLFN learning

Each SLFN learning consists of an input layer, a hidden layer with dipole topology neurons, and an output layer of linear weights, which is denoted as,

$$\boldsymbol{H}\boldsymbol{\beta} = \boldsymbol{O} \tag{6}$$

$$\mathbf{H}(\boldsymbol{a}_{11}, \boldsymbol{a}_{21}, \ldots, \boldsymbol{a}_{\tilde{Q}1}, \boldsymbol{a}_{12}, \boldsymbol{a}_{22}, \ldots, \boldsymbol{a}_{\tilde{Q}2}, b_1, b_2 \ldots, b_{\tilde{Q}}, \boldsymbol{I}_1, \ldots, \boldsymbol{I}_Q)$$
$$= \begin{bmatrix} K(\boldsymbol{I}_1, \boldsymbol{a}_{11}, \boldsymbol{a}_{12}, b_1) & K(\boldsymbol{I}_2, \boldsymbol{a}_{11}, \boldsymbol{a}_{12}, b_1) & \cdots & K(\boldsymbol{I}_Q, \boldsymbol{a}_{11}, \boldsymbol{a}_{12}, b_1) \\ \vdots & \vdots & \vdots & \vdots \\ K(\boldsymbol{I}_1, \boldsymbol{a}_{\tilde{Q}1}, \boldsymbol{a}_{\tilde{Q}2}, b_{\tilde{Q}}) & K(\boldsymbol{I}_2, \boldsymbol{a}_{\tilde{Q}1}, \boldsymbol{a}_{\tilde{Q}2}, b_{\tilde{Q}}) & \cdots & K(\boldsymbol{I}_Q, \boldsymbol{a}_{\tilde{Q}1}, \boldsymbol{a}_{\tilde{Q}2}, b_{\tilde{Q}}) \\ K(\boldsymbol{I}_2, \boldsymbol{a}_{11}, \boldsymbol{a}_{12}, b_1) & K(\boldsymbol{I}_3, \boldsymbol{a}_{11}, \boldsymbol{a}_{12}, b_1) & \cdots & K(\boldsymbol{I}_1, \boldsymbol{a}_{11}, \boldsymbol{a}_{12}, b_1) \\ \vdots & \vdots & \vdots & \vdots \\ K(\boldsymbol{I}_2, \boldsymbol{a}_{\tilde{Q}1}, \boldsymbol{a}_{\tilde{Q}2}, b_{\tilde{Q}}) & K(\boldsymbol{I}_3, \boldsymbol{a}_{\tilde{Q}1}, \boldsymbol{a}_{\tilde{Q}2}, b_{\tilde{Q}}) & \cdots & K(\boldsymbol{I}_1, \boldsymbol{a}_{\tilde{Q}1}, \boldsymbol{a}_{\tilde{Q}2}, b_{\tilde{Q}}) \end{bmatrix}'_{2\tilde{Q}\times Q}$$
$$\boldsymbol{\beta} = \begin{bmatrix} \boldsymbol{\beta}_1 & \cdots & \boldsymbol{\beta}_{\tilde{Q}} & \boldsymbol{\beta}_{\tilde{Q}+1} & \cdots & \boldsymbol{\beta}_{2\tilde{Q}} \end{bmatrix}'_{N\times 2\tilde{Q}}, \quad \mathbf{O} = \begin{bmatrix} \boldsymbol{O}_1 & \cdots & \boldsymbol{O}_q & \cdots & \boldsymbol{O}_Q \end{bmatrix}'_{N\times Q}$$

The steps for ELM learning are shown in Fig. 2.

Here, the hidden node number $\tilde{Q}$ is chosen by maintaining the same principle as the original ELM learning, which is thereby set as $2\tilde{Q} \ll Q$.

4.2 ELM ensemble

ELM ensemble is further set up here to improve generalization performance, with every 3D object an individual SLFN. The idea of ELM ensemble is to generate multiple versions of optimal cognition from sorts of 2D images, which when combined, will provide more stable interpretation about a given 3D object.

The learning process in the ELM ensemble takes two steps, i.e., training a collection of SLFNs for multiple 3D objects and then combining all the individual predictions. The combination strategy here is taken as a linearly weighted summation of the individual outputs, i.e., $Y = \sum_{n=1}^{N} \omega_n Y_n$, where Y_n is the output of the nth SLFN, and ω_n corresponds to the combination weight, with $\sum_{n=1}^{N} \omega_n = 1$. In this case, the output of each individual can be pruned to $Y_n \in \mathrm{R}$ for simplification, and the combination weights could all set to be equal when 2D images from every 3D object make the same contribution to the optimal cognition course. The architecture of one ELM ensemble is shown as Fig. 3.

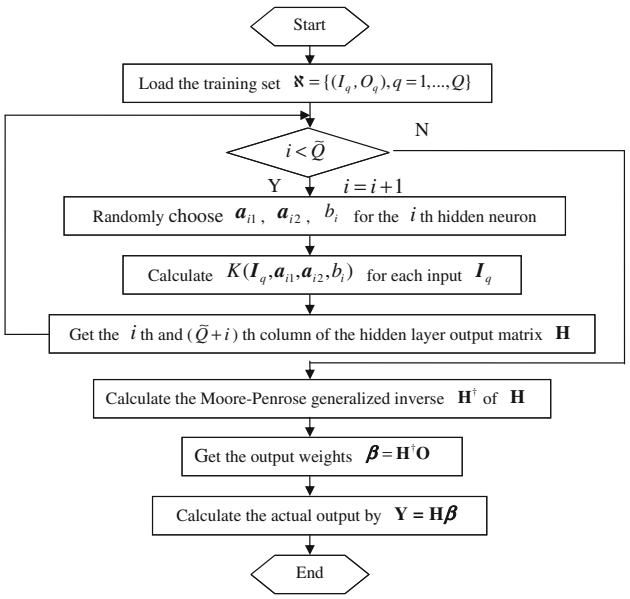

Fig. 2 The flow chart of ELM learning

5 Simulation result analysis

The simulations were taken on the image database from (a) to (d) listed in Table 1, which consists of 2D images covering the visual sphere surrounding 3D objects, as is shown in Fig. 4. The viewpoint variation of every two adjoining images is around at 5° through 360°. For each view angle, an optional transformation was undergone

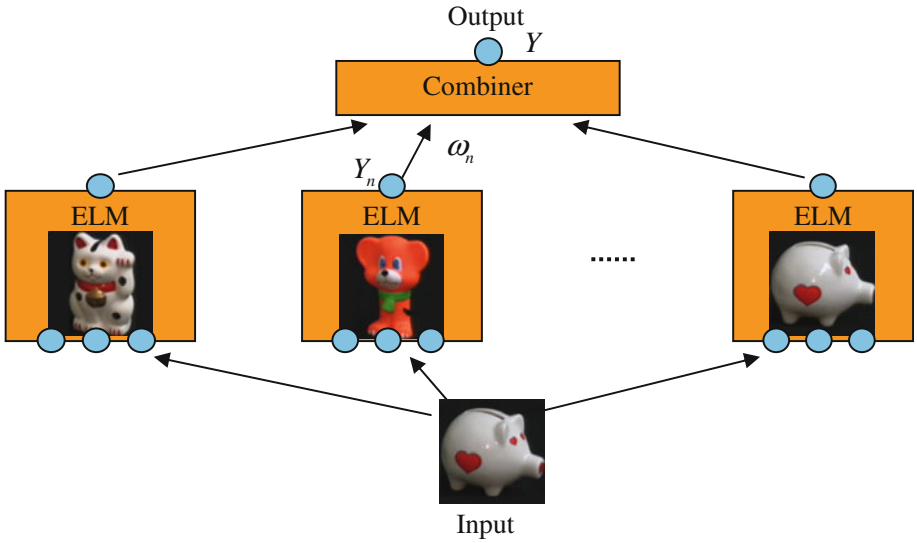

Fig. 3 The architecture of an ELM ensemble

Table 1 Specification of database

Database		Training samples	Testing samples	Samples per object	Classes
(a)	Animals	288	864	72	16
(b)	Fruit and vegetables	504	1,512	72	28
(c)	Toys 1	108	324	72	6
(d)	Toys 2	702	2,106	72	39

Fig. 4 Example images from the database

to make sure invariance under translation, rotation, and scale in the frame [11, 28]. Only a quarter of 2D images were chosen from the original database for the training set and the rest constitute the test set. When employing distinct SLFNs with BP or ELM algorithm, taking the sigmoid function, the radial basis function, the dipole topology function as the activation function, setting the number of hidden layer nodes uniformly as 50 in each SLFN and conducting 5 trials for each case, the performance comparison on the training time, the test time, the training success rate, the test success rate, and the standard deviation, is, respectively, shown in Table 2. Taking the database (c) as an example, the increase in the number of the hidden layer nodes from 50 to 100 brought approximately twice as much as the computation and time consuming. However, there are no obvious improvements or even deceases in the recognition performance. In our future work, we will further explore the effects and the model selection of the number of hidden layer nodes [29] in the developed approach.

6 Conclusions

In this paper, we have presented a scheme of 3D object recognition based on the optimal cognition principle. For each 3D object, we have built one individual SLFN as a fine and easy realization to the geometrical topology hypothesis along multiple view angles, and ELM algorithm has been taken to develop the relevant mathematical criterion correspondingly. The dipole topology model has

Table 2 Performance comparison

Datasets	Performances		SLFN			
			BP Sigmoid	ELM Sigmoid	ELM RBF	ELM Dipole
(a)	Training	Time(s)	602.501	12.769	267.161	708.531
		Success rate (%)	94.8	93.4	99.3	99.8
		SD	1.091	1.653	0.495	0.589
	Testing	Time(s)	0.024	0.035	0.867	2.238
		Success rate (%)	88.5	88.4	96.9	97.2
		SD	2.672	4.384	2.192	1.384
(b)	Training	Time(s)	882.877	31.047	744.406	1977.516
		Success rate (%)	99.4	98.3	91.9	99.3
		SD	1.531	2.728	6.097	1.795
	Testing	Time(s)	0.075	0.051	1.463	4.000
		Success rate (%)	88	87	85.2	94.4
		SD	3.973	4.799	6.573	3.812
(c)	Training	Time(s)	189.188	5.359	92.047	115.688
		Success rate (%)	94.3	100	100	100
		SD	5.213	0	0	0
	Testing	Time(s)	0.022	0.017	0.771	0.991
		Success rate (%)	87.8	78.3	98.3	100
		SD	7.5816	9.464	3.712	0
(d)	Training	Time(s)	1229.507	55.406	1425.703	3839.516
		Success rate (%)	83.3	82.0	82.7	98.7
		SD	5.942	7.212	6.930	3.172
	Testing	Time(s)	0.106	0.066	2.004	5.559
		Success rate (%)	76.9	61.8	76.5	82.4
		SD	8.791	10.383	5.34	4.98

been established to estimate the inherent dependence of a local topological segment in high-dimensional space. ELM ensemble has been then used to organize the individual SLFNs into combination. The simulation results have shown the good performance, the effectiveness, and the feasibility of the proposed approach.

Acknowledgments This work was partially supported by the Natural Science Foundation of P. R. China (41176076), the National High Technology Research and Development Program of P. R. China (2006AA09Z231), the Science and Technology Development Program of Shandong Province (2008GG1055011, BS2009HZ006), and the Science and Technology Development Program of Qingdao (103413jch).

References

1. Clark A (2001) Mindware: an introduction to the philosophy of cognitive science. Oxford University Press, New York
2. Shimshoni I, Ponce J (2000) Probabilistic 3D object recognition. Int J Comput Vis 36(1):51–70
3. Ma Y, Soatto S, Kosecka J, Sastry S (2003) An invitation to 3-D vision: from images to geometric models. Springer, New York
4. Pope AR, Lowe DG (2000) Probabilistic models of appearance for 3-D object recognition. Int J Comput Vis 40(2):149–167
5. Cyr CM, Kimia BB (2004) A similarity-based aspect-graph approach to 3D object recognition. Int J Comput Vis 57(1):5–22
6. Javed O, Shah M, Comaniciu D (2004) A probabilistic framework for object recognition in video. International Conference on Image Processing, Singapore
7. Fisher RA (1952) Contributions to mathematical statistics. Wiley, New York
8. Haykin S (1999) Neural networks: a comprehensive foundation. Prentice-Hall, New Jersey
9. Verleysen M, Voz JL, Thissen P, Legat JD (1995) A statistical neural network for high-dimensional vector classification. IEEE international conference on neural networks, ICNN'95, Perth, pp 990–994
10. Huang D-S (1996) Systematic theory of neural networks for pattern recognition. Publishing House of Electronic Industry of China, Beijing, pp 70–78
11. Nian R, Ji G-R, Zhao W-C, Feng C (2007) Probabilistic 3D object recognition from 2D invariant view sequence based on similarity. Neurocomputing 70(4–6):785–793
12. Vapnik VN (1995) The nature of statistical learning theory. Springer, Berlin
13. Xu L (2002) Bayesian Ying Yang harmony learning. In: Arbib MA (ed) The handbook of brain theory and neural networks. The MIT Press, Cambridge
14. Wang S-J (2003) Biomimetics pattern recognition. INNS, ENNS, JNNS Newletters Elseviers

15. Nian R, Ji G-R, Zhao W-C, Feng C (2005) ANN hybrid ensemble learning strategy in 3D object recognition and pose estimation based on similarity. Advances in Intelligent Computing, LNCS 3644, ICIC, part 1, pp 650–660
16. Huang G-B, Zhu Q-Y, Siew C-K (2006) Extreme learning machine: theory and applications. Neurocomputing 70:489–501
17. Huang G-B, Ding X, Zhou H (2010) Optimization method based extreme learning machine for classification. Neurocomputing 74:155–163
18. Man ZH, Lee K, Wang DH, Cao ZW, Miao CY (2011) A modified ELM algorithm for single-hidden layer feedforward neural networks with linear nodes. 2011 6th IEEE conference on industrial electronics and applications (ICIEA), pp 2524–2529
19. Miche Y, Sorjamaa A, Bas P, Simula O, Jutten C, Lendasse A (2010) Optimally-pruned extreme learning machine. IEEE Trans Neural Netw 21:158–162
20. Huang G-B (2003) Learning capability and storage capacity of two hidden-layer feedforward networks. IEEE Trans Neural Netw 14(2):274–281
21. Verleysen M (2003) Learning high-dimensional data. In: Ablameyko S et al (eds) Limitations and future trends in neural computation. IOS Press, Amsterdam, pp 141–162
22. Wang S-J, Wang B-N (2002) Analysis and theory of high-dimension spatial geometry for artificial neural networks. Acta Electron Sinica 30(1):1–4
23. Aupetit M (2007) Visualizing distortions and recovering topology in continuous projection techniques. Neurocomputing 70(7–9): 1304–1330
24. Aupetit M (2005) Learning topology with the generative gaussian graph and the EM algorithm. NIPS, Vancouver
25. Ji G-R, Nian R, Yang S-M, Zhou L-J, Feng C (2006) Cellular recognition for species of phytoplankton via statistical spatial analysis. Lecture Notes in Control and Information Sciences, ICIC, pp 761–766
26. Koenderink JJ, van Doorn AJ (1976) The singularities of the visual mapping. Biol Cyber 24:51–59
27. Basri R, Weinshall D (1996) Distance metric between 3D models and 2D images for recognition and classification. IEEE Trans Pattern Anal Mach Intell 18(4):465–470
28. Casasent DP, Neiberg LM (1995) Classifier and shift-invariant automatic target recognition neural networks. Neural Netw 8(7–8):1117–1129
29. Lendasse A, Wertz V, Verleysen M (2003) Model selection with cross-validations and bootstraps—application to time series prediction with RBFN models. ICANN 2003, Joint international conference on artificial neural networks, Istanbul (Turkey), volume 2714, pp 573–580